Results of the Pierre Auger Observatory - aspects related to hadronic interaction models

Petr Travnicek for the Pierre Auger Collaboration[†]
Institute of Physics of the Academy of Sciences of the Czech Republic, Na Slovance 2 CZ-182 21 Praha 8, Czech Republic

DOI: http://dx.doi.org/10.3204/DESY-PROC-2009-01/73

Abstract

The southern part of the Pierre Auger Observatory in Argentina is now fully completed and already provides world unique data samples of the cosmic ray showers in the energy range from 10^{18} eV till above 10^{20} eV. In order to avoid a strong dependency on MC simulations for energy calibration, the experiment combines two techniques: surface detector arrays and fluorescence telescopes. However, the interpretation of some measured quantities such as mean shower maximum in terms of chemical composition of cosmic rays, naturally depends on MC simulations and models of hadronic interactions at extremely high energies. This contribution describes selected results of the Pierre Auger Observatory and pinpoints several issues where the models of hadronic interactions play a very important role or can be even tested at energies far from the reach of current accelerators.

1 Introduction

The existence of Ultra High Energy Cosmic Rays (UHECR) is difficult to explain either by present scenarios of acceleration mechanisms in astronomical objects or by models suggesting that these particles originate e.g. from decays of super-heavy dark matter. UHECR thus attract attention of both astrophysicists and particle physicists.

UHECR are supposed to be mostly protons or heavier nuclei that quickly lose energy as they interact with relict photons at energies above the pion production threshold $E_{TH} \sim 6\times10^{19}$ eV (GZK mechanism [1]). Consequently, events observed when the particles hit the Earth atmosphere have to originate from distances close to us (within $\sim$ 100 Mpc) and the flux of these particles has to be suppressed above the GZK threshold. This expectation is however in contradiction with previous measurements of the AGASA experiment [2]. All the above-mentioned mysteries of UHECR and more that were presented e.g. in Ref. [3] were the basic motivations for construction of the Pierre Auger Observatory (PAO), the world largest cosmic ray detector.

Already during the construction phase the PAO was able to take data and the collaboration reported many results such as an estimate of upper limit on the cosmic-ray photon and diffuse tau neutrino flux [4–6] or the highlighted analysis of correlation of the highest-energy cosmic rays with the positions of nearby active galactic nuclei [7, 8]. In this contribution we rather focus

[†] see `www/auger.org/admin` for full author list

on energy calibration, spectrum and composition studies and examples how PAO can test the validity of hadronic interaction models at extreme energies.

2 Experimental setup and measurement principle

The southern site of the PAO is situated in the Argentinian province Mendoza, close to the city of Malargüe. It consists of 3000 km^2 surface detector arrays and a set of 24 fluorescence telescopes. The surface detector stations are water Cerenkov tanks each equipped by 3 photomultipliers. Six fluorescence telescopes occupy one fluorescence detector building. In total four of these buildings are located on the array border on small hills and thus overlook the interior of the array. In the year 2008 the southern part of the Observatory was fully completed with successful operation of all four fluorescence detector buildings and by fulfilling the original aim of 1600 deployed and working surface detector stations.

The essential part of the project is to build the northern counterpart of the existing south experiment. The suitable site was already chosen in Colorado, USA. Not only the full sky coverage but also the interesting and encouraging results obtained from the southern site and subsequent new scientific questions emerging from the data are the main motivations for the northern Observatory.

When a cosmic ray particle hits the Earth atmosphere, it interacts at high altitudes with a nucleus of the atmospheric gas and many new particles are created in the forward direction. Secondary particles then continue to interact with other atmospheric nuclei and the extensive air shower is formed. Decays of secondary neutral pions feed the electromagnetic shower and decays of charged mesons form the muon component. The surface array measures the shower lateral profile on the ground and surface detector stations are sensitive to both electromagnetic and muon components. The fluorescence telescopes register the longitudinal profile of the fluorescence light induced along the air shower by de-excitations of N_2 molecules excited by the passage of the electromagnetic shower. The measured light intensity is proportional to the energy that shower particles lose in the atmosphere. The fluorescence detectors thus provide calorimetric measurement of the shower energy estimated as $E_{FD} = k \int_0^\infty \frac{dE}{dX} dX$, where X is the atmospheric depth and k is the correction factor taking into account missing energy due to neutrinos and energetic muons. Fluorescence telescopes can, however, operate only during the nights with low Moon-light intensity. Since the majority of the measured showers is detected only by surface Cerenkov stations, the conversion of the surface detector signal to shower energy has to be used for these events.

3 Energy calibration of surface detector signals and cosmic ray energy spectrum

The signal at about 1000 m from the shower core (S(1000)) is on average the ideal parameter to measure the shower energy from the surface detector data [9] . The chosen distance to shower core is mostly given by the requirement of good reconstruction quality and it is defined by the geometry of the array. Having the optimal energy estimator determined, the correction to the signal attenuation for different zenith angles has to be estimated. This is done from the real data avoiding any Monte Carlo simulations. For each shower the signal parameter S38=S(1000)/CIC(θ) is calculated. This parameter is defined as the S(1000) signal of the same shower if its zenith

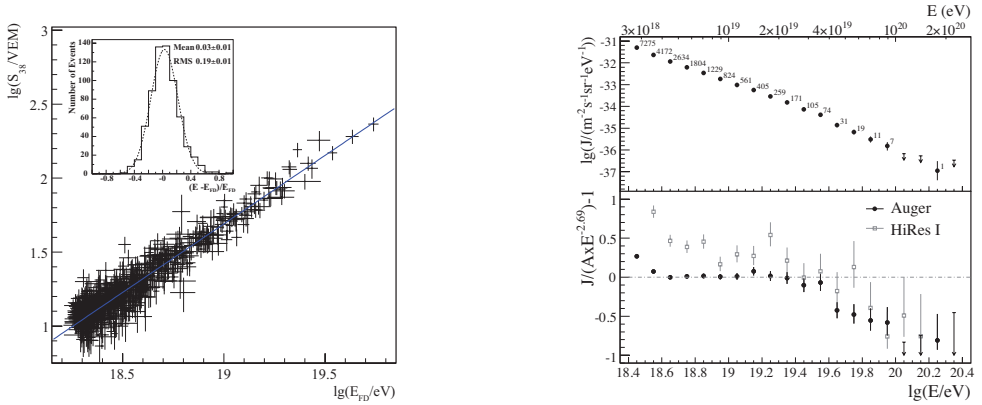

Fig. 1: *(left)* Correlation between $\lg S_{38^\circ}$ and $\lg E_{FD}$ for the 661 hybrid events used in the fit. The full line is the best fit to the data. The fractional differences between the two energy estimators are shown in the inset. *(right)* Upper panel: The differential flux J as a function of energy, with statistical uncertainties. Lower Panel: The fractional differences between Auger and HiResI data compared with an energy spectrum $J \sim \mathrm{E}^{-2.69}$.

angle θ would be 38°. The crucial part is thus to estimate the signal attenuation curve CIC(θ) from the real data. This is done by requiring the isotropic distribution of the events above a given energy (i.e. above a given S38). Since the surface detector is flat and the trigger efficiency approaches unity (>99%) above 3×10^{18} eV it is natural to expect that the distribution of number of events above some energy is flat in $\cos^2(\theta)$. The constant intensity cut given in the number of events in each $\cos^2(\theta)$ bin is chosen and the CIC(θ) is then found from the real data so that the dN/d($\cos^2(\theta)$) is constant as required. It was shown that the shape of the CIC(θ) curve does not depend on the chosen value of the cut.

At this stage the last step of the energy calibration is applied. It is the relation of the S38 parameter to the measured energy from the fluorescence detectors. The calibration curve is shown in Fig. 1 (left) showing nice correlations of the two parameters. The correction to the missing energy applied to the measured calorimetric energy of the fluorescence detectors is the only step where the models of hadronic interaction enter the calibration procedure. The differences between the corrections for different models and primaries are on the level of a few percent [10]. The total uncertainty of the fluorescence energy measurement is about 22%. While the largest part is given by the uncertainty of fluorescence yield (15 %), the missing energy uncertainty is only about 4 %.

Having the conversion of S(1000) to S38 and finally to the shower energy estimated, the cosmic ray energy spectrum can be constructed [11]. The spectrum is plotted in Fig. 1 (right) together with the HiResI data [12]. At the confidence level of 6 standard deviations the flux $J \sim E^{\alpha=-2.69}$ stops to continue with the same slope α above the energy 4×10^{19} eV.

4 Mass composition, shower maximum

While the estimated energy spectrum depends only slightly on the models of hadronic interactions, the analyzes of cosmic ray composition are essentially based on these models. In order

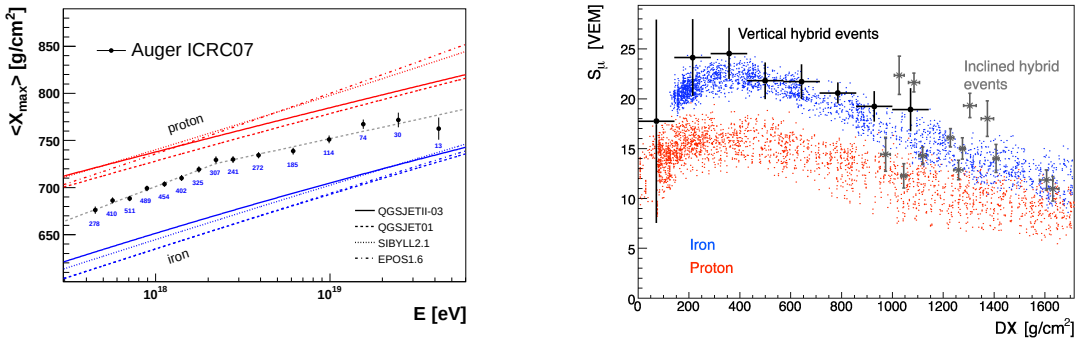

Fig. 2: *(left)* $< X_{max} >$ as a function of energy compared to predictions from hadronic interaction models. The dashed line denotes a fit with two constant elongation rates (slopes k of $< X_{max} > \sim k \lg(E/eV)$) and a break-point. *(right)* Reconstructed and predicted (energy scale $E_{MC} = 1.3 E_{\rm FD}$) muon tank signal contribution in dependence on the distance of the shower maximum to ground for vertical and inclined hybrid events.

to obtain information about the composition of comic rays, the PAO studies shower parameters sensitive to the mass of the primary particle. One of the most powerful parameters is the position of the shower maximum measured by the fluorescence detectors.

As the shower passes through the atmosphere, the electromagnetic component evolves and increases its size until the particle energy is lower than critical energy in the air. At this point the shower reaches its maximum and this position is defined as the amount of traversed matter X_{max}. The shower initiated by heavy nucleus with N nucleons can be roughly approximated as N proton sub-showers at energies N times lower. These sub-showers thus penetrate less the atmosphere than the proton shower at the same total energy resulting to smaller average X_{max} value. Also the shower to shower fluctuations of X_{max} would be smaller for the heavy primary particle because the "averaging" occurs between these N sub-showers. The average value of X_{max} is related to the mean logarithmic mass via: $< X_{max} >= D_{\rm p}[\ln(E/E_0) - < \ln A >] + {\rm c}_p$, where $D_{\rm p}$ denotes the 'elongation rate' of a proton, and ${\rm c}_p$ is the average depth of a proton with reference energy E_0.

The dependency of the average measured X_{max} on energy is plotted in Fig. 2 (left) with the prediction of various interaction models [13]. The measurements favor a mixed composition at all energies. However, a more precise interpretation of Fig. 2 in terms of chemical composition is ambiguous due to uncertainties of hadronic interactions. At low energies the data suggests moderate lightening of primary cosmic rays. At high energies EPOS model seems to favor transition from the light to the heavy component. When compared to QGSJETII model, the experimental data seem to follow an almost constant composition in the same energy region.

5 Tests of hadronic interaction models

Since for the composition analysis the knowledge of hadronic interactions is essential, the question appears, whether and how the interaction models can be tested using the data.

One of the possible tests [14] requires the assumption of so called shower universality of the electromagnetic component. It is based on the natural expectation that due to huge amount of

particles in the shower, the details of the initial hadronic interaction are quickly washed out. The resulting electromagnetic component can be thus parametrized using global shower parameters such as energy, zenith angle and distance of the detector to shower maximum. It was shown that to the level of about 15% the signal from the electromagnetic component at given distances to shower maximum is in fact same for proton and iron primary particles as well as for different interaction models [14].

For the muon signal the situation is quite different and showers initiated by heavier primaries at given energy yield larger muon signals than those originated by light primaries. However, it is important that the ratio of the signal for a combination of given model and primary particle to some reference prediction (e.g. for protons in QGSJETII model) is constant as a function of the distance to the shower maximum. This leads to the parametrization of the total signal in terms of the equation:

$$S_{MC}(E,\theta,DX,N_{\mu}^{REL}) = S_{EM}(E,\theta,DX) + N_{\mu}^{REL} S_{\mu}^{QGSJETII,p}(10^{19}eV,\theta,DX),$$

where DX is distance of the detector to the shower maximum, θ is the zenith angle, E is energy of the primary particle and N_{μ}^{REL} is the relative muon normalization with respect to the prediction of the QGSJETII model at $10^{19}eV$ for protons. The constant intensity method similar to what was already described is section 3 can be used to find the muon normalization factor so that the distribution of real events satisfies:

$$\frac{dN}{d(\cos^2(\theta))}_{S(1000)>S_{MC}(E,\theta,DX,N_{\mu}^{REL})} = const.$$

In other words, the question is asked, how the Monte Carlo simulations have to be modified in terms of N_{μ}^{REL} so that the predicted attenuation curve is the same as the attenuation curve measured.

For the bulk of the surface detector events the position of the shower maximum is unknown and the measured $< X_{max} >$ as described in Sec. 4 must be taken and $DX = X_{GR}\sec(\theta) - - < X_{max} >$, where X_{GR} is the vertical atmospheric depth of the ground position. S_{MC} is then function of only 3 parameters, $S_{MC} = S_{MC}(E,\theta,N_{\mu}^{REL})$. The shower to shower fluctuations of X_{max} are taken into account at the end of the analysis. It was shown that $N_{\mu}^{REL} = 1.45 \pm 0.11(\mathrm{stat})^{+0.11}_{-0.09}(\mathrm{sys})$ [15]. About 50 % more muons are thus needed so that proton primaries with QGSJETII model simulate properly the measured signal attenuation. The prediction of the same model but with iron nuclei gives $N_{\mu}^{REL} \sim 1.39$ with respect to the proton prediction. Hence, either the muon numbers in the model have to be adjusted or particles as heavy as iron or even heavier form the entire primary particle flux (which is quite improbable and also contradicts the shower maximum studies presented in Sec. 4). The advantage of this method is that after N_{μ}^{REL} is found the energy scale $S38_{MC}(10^{19}eV, 38^{\circ}, N_{\mu}^{REL} = 1.45)$ can be estimated. A 30% shift between the FD and Monte Carlo energy scale was found [15].

Other model tests can be done with smaller statistics on hybrid events where the shower profile is measured by the fluorescence detector (so the energy and X_{max} are known). The muon signal can be then calculated as a difference of the measured signal in the surface detectors and the electromagnetic signal recorded by fluorescence telescopes.

Also inclined events can be analyzed. The electromagnetic signal of these showers on ground is marginal and the measured surface detector signal is caused directly by the muons. Both analyzes agree with the value N_{μ}^{REL} obtained from the constant intensity method. The evolution of the muon signal as a function of the distance to the shower maximum for hybrid and inclined events is plotted in Fig.2 (right) together with the prediction of the QGSJETII model [15].

6 Conclusions

The hybrid approach of the PAO means that the crucial results such as the energy spectrum or anisotropy studies are independent on models of hadronic interactions. However, these models are essential to interpret shower parameters sensitive to primary particle mass in terms of the UHECR composition. Many magnitudes above the energy of current accelerators, the models of hadronic interaction can be tested using the data of the PAO.

Acknowledgments

The author would like to thank D. Nosek, T. Pierog, R. Smida, F. Schmidt and J.Ridky from the Pierre Auger collaboration for their comments and help with preparation of the contribution. The contribution was prepared with the support of grants of the Czech Republic GACR 202/06/P006, MSMT-CR LA08016 and MSMT-LC527.

References

[1] K. Greisen, Phys. Rev. Lett. **16** (1966) 748.
G. T. Zatsepin and V. A. Kuzmin, JETP Lett. **4** (1966) 78 [Pisma Zh. Eksp. Teor. Fiz. **4** (1966) 114]. .

[2] M. Takeda *et al.*, Phys. Rev. Lett. **81** (1998) 1163 .

[3] H Meyer, these proceedings, "Cosmic Rays and high energy collisons at HERA, Tevatron and LHC" .

[4] J. Abraham *et al.* [Pierre Auger Collaboration], Astropart. Phys. **27** (2007) 155 .

[5] J. Abraham *et al.* [Pierre Auger Collaboration], Astropart. Phys. **29** (2008) 243 .

[6] J. Abraham *et al.* [The Pierre Auger Collaboration], Phys. Rev. Lett. **100** (2008) 211101 .

[7] J. Abraham *et al.* [Pierre Auger Collaboration], Science **318** (2007) 938 .

[8] J. Abraham *et al.* [Pierre Auger Collaboration], Astropart. Phys. **29** (2008) 188 [Erratum-ibid. **30** (2008) 45] .

[9] D. Newton, J. Knapp and A. A. Watson, Astropart. Phys. **26** (2007) 414 [arXiv:astro-ph/0608118]. Phys. Rev. Lett. **101** (2008) 061101 .

[10] T. Pierog, R. Engel, D. Heck, S. Ostapchenko and K. Werner, P roceedings of the 30th International Cosmic Ray Conference (ICRC 2007), Merida, Yucatan, Mexico, 3-11 Jul 2007. arXiv:0802.1262 [astro-ph] .

[11] J. Abraham *et al.* [Pierre Auger Collaboration], Phys. Rev. Lett. **101** (2008) 061101 .

[12] R.U. Abbasi *et al.* , Phys. Rev. Lett. **100**, 10 1101 (2008) .

[13] M. Unger [The Pierre Auger Collaboration], arXiv:0706.1495 [astro-ph]. Proceedings of the 30th International Cosmic Ray Con ference (ICRC 2007), Merida, Yucatan, Mexico, 3-11 Jul 2007 .

[14] F. Schmidt, M. Ave, L. Cazon and A. S. Chou, Astropart. Phys. **29** (2008) 355 .

[15] R. Engel [Pierre Auger Collaboration], Proceedings of the 30th International Cosmic Ray Conference (ICRC 2007), Merida, Yucatan, Mexico, 3-11 Jul 2007.

.